Photochemistry of HNCO in Solid Xenon: Photoinduced and Thermally Activated Formation of HXeNCO†

Mika Pettersson,* Leonid Khriachtchev, Jan Lundell, Santtu Jolkkonen, and Markku Räsänen

Laboratory of Physical Chemistry, P.O. Box 55, FIN-00014 University of Helsinki, Finland

Received: October 14, 1999; In Final Form: December 23, 1999

The preparation and characterization of a novel rare-gas-containing compound HXeNCO in solid Xe is described. HXeNCO is formed in two ways. Photolysis of HNCO at 193 nm in solid Xe directly produces HXeNCO providing the first experimental evidence of direct photoinduced formation of a HXY-type rare-gas compound (X = Xe, Kr; Y is an electronegative fragment), which can be attributed to relatively high photostability of HXeNCO. This finding particularly shows that the HXY compounds can be intermediates in the photolysis of HY in the presence of X. The amount of HXeNCO produced initially in photolysis of HNCO remains small because HXeNCO decomposes under irradiation. More efficient production of HXeNCO is achieved in the thermal reaction H + Xe + NCO → HXeNCO after photolysis of HNCO. HXeNCO has two strong IR absorptions: the asymmetric NCO stretch at 2148.3 cm^{-1} and the Xe−H stretch at 1788.1 cm^{-1}. The assignment is supported by the deuteration experiments and the ab initio calculations. HXeNCO decomposes at 405 nm irradiation producing HNCO and (H + NCO).

1. Introduction

Xenon cannot be considered very inert as evidenced by a large number of xenon-containing compounds synthesized during the last four decades.[1] Recently, we have used the matrix-isolation method to synthesize and investigate a number of novel rare-gas hydrides.[2−7] These compounds are of the HXY type where X is Xe or Kr and Y is the fragment with a relatively large electron affinity. The first observed HXY compounds were triatomic HXeCl, HXeBr, HXeI, HXeH, and HKrCl.[2,3] After understanding mechanism of their formation[8] and the nature of bonding, the ideas were tested to prepare more complex compounds, and this led to characterization of HXeCN, HXeNC, HKrCN, HXeSH, and HXeOH.[4,5,7] Since the NCO radical has a large electron affinity (3.6 eV)[9] like halogens and CN, HXeNCO is probably a stable compound as well, and this study was designed to test this hypothesis. In this connection, it is interesting to note that the analogous fluorine compound, FXeNCO, is computationally stable and it was recently claimed to be formed as an intermediate in a reaction between XeF_2 and NaOCN.[10]

While our series of studies is focused on creating new rare-gas compounds with novel bonds and to understand their vibrational and structural features, we also gain insight into the dynamical processes connected with their formation. This applies especially to photolysis of small hydrides used as precursors in these experiments, as well as to both photoinduced and thermal atomic mobility in rare-gas solids. Photodissociation of small hydrides in rare-gas solids has recently been a quite popular topic because it provides a model system for understanding condensed phase photodynamics.[11−16] Direct involvement of HXY in photodissociation dynamics of HY in solid X has been suggested.[17] In fact, the whole event of photodissociation of HY in solid X can be contributed by a photoisomerization process of HY/X to HXY with the following photodecomposition of HXY. Therefore, any realistic modeling of the photodissociation should take into account the HXY configuration. Even in the case of photodissociation of a binary HY···X complex the existence of a deep well in a HXY configuration might have an effect on the dynamics of the whole system. However, although photodynamics of various systems consisting of hydrogen halides and rare gases were studied theoretically, these effects were not taken into account.[18−22] On the other hand, there is no previous experimental evidence of the creation of HXY compounds directly in photolysis of HY and the formation of HXY so far has required thermal mobilization of hydrogen atoms in the matrix.[2−7]

In a recent study, we have investigated photochemistry of HNCO in solid Xe.[23] It was found that both HNCO → HN + CO and HNCO → H + NCO channels are open in Xe matrices leading to isolation of NCO, NH, CO, NH−CO complexes, and H atoms after photolysis. Further irradiation induces fragmentation of NCO mostly into (NO + C) but also into (NC + O). Annealing at ∼50 K after photolysis produces previously known HCO, HXeH, HXeCN, HXeNC, and additionally the H_2NCO radical, which was directly observed for the first time.

In this paper, we continue our experiments with rare-gas compounds of the type HXY by introducing a new member of this family, HXeNCO. The synthesis of this molecule generally follows the recipe used for the other HXY compounds previously: photodissociation of HNCO to H + NCO followed by thermal mobilization of hydrogen atoms and subsequent formation of HXeNCO in the reaction H + Xe + NCO → HXeNCO. Importantly, HXeNCO is also formed directly during photolysis, which shows that HXeNCO is an important intermediate in the photolysis process.

2. Experimental Details

HNCO was synthesized from cyanuric acid (Merck, 99.5%) as described in ref 23. Xenon (99.997%, AGA) was used without further purification. The matrices were prepared by depositing a premixed HNCO/Xe gas onto a CsI substrate. A gas ratio of 1:2000 and deposition temperature of 30 K produced highly

† Part of the special issue "Marilyn Jacox Festschrift".

* Corresponding author. E-mail: petters@csc.fi.

10.1021/jp9936751 CCC: $19.00
Published on Web 03/31/2000

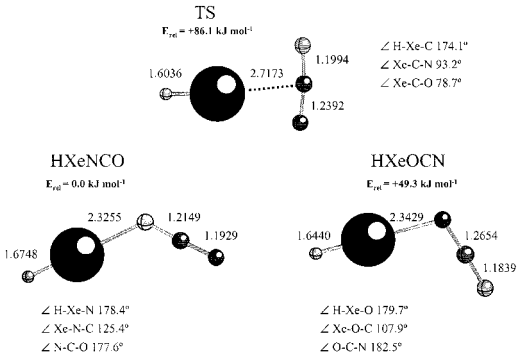

Figure 1. Computed structures of HXeNCO, HXeOCN, and the transition state between them at the MP2/LJ18/6-311++G(2d,2p) level of theory.

monomeric matrices. After deposition, the samples were cooled to 7.5 K and the photolysis was carried out at this temperature.

HNCO was photolyzed by an excimer laser (ELI 76, Estonian Academy of Sciences) operating at 193 nm, the fourth harmonic (266 nm) of a Nd:YAG laser (Powerlite, Continuum) or doubled radiation of an optical parametric oscillator (OPO Sunlite with FX-1, Continuum). These sources deliver radiation typically with pulse duration of 5−10 ns and pulse energy of ∼10 mJ. The pulse energies were measured by a laser power meter (MAX 5200, Molectron). The IR absorption spectra were recorded by a Nicolet 60 SX spectrometer with a resolution of 1 or 0.25 cm^{-1}.

3. Computational Details

The calculations were performed with the Gaussian 98 package of computer codes.[24] Electron correlation was considered via Møller−Plesset perturbation theory to the second order (MP2). For xenon, the effective quasirelativistic core potential (ECP) by LaJohn and co-workers was used.[25] The formalism of this LJ18 ECP involves 18 valence electrons, and the valence basis set was used in a decontracted form. For all other atoms the standard Pople-type 6-311++G(2d,2p) basis set was employed.

4. Computational Results

Figure 1 presents the structures of HXeNCO, HXeOCN, and the transition state between them computed at the MP2/LJ18/6-311++G(2d,2p) level. From these two isomers, HXeNCO is the lowest in energy and HXeOCN is about 50 kJ/mol higher in energy. The isomerization between these two forms occurs via rotation of NCO fragment involving a T-shaped transition state with a relative energy of 86 kJ mol^{-1}.

The computed vibrational spectra of HXeNCO and HXeOCN are presented in Table 1. For HXeNCO, the calculations predict two very strong bands which can be identified as the asymmetric NCO and Xe−H stretching modes, and intensities of the other modes are about 2 orders of magnitude smaller. The shift of ν_{as}(NCO) upon deuteration is predicted to be 11 cm^{-1}, which should be well observable experimentally. For HXeOCN, ν_{as}-(OCN) is predicted to be much weaker than the Xe−H stretch and the energy difference between these two modes is only about 70 cm^{-1}. Additionally, HXeOCN should have a band at about 1140 cm^{-1} of the similar intensity as the asymmetric OCN stretch. Our experience shows that at this level of theory the position of Xe−H stretch is somewhat overestimated.[6] When we use the empirical relation between the experimental and predicted values at this computational level for the other similar molecules[26]

$$\nu(\text{exp}) = 1.335\nu(\text{calc}) - 881\ \text{cm}^{-1} \quad (1)$$

we can estimate that the Xe−H stretches for HXeNCO and HXeOCN should be at about 1770 and 1950 cm^{-1}, respectively.

5. Experimental Results

The details of spectroscopy and photolysis channels of HNCO in solid Xe are reported in our previous paper[23] and here we concentrate only on results concerning HXeNCO. The HNCO → H + NCO photolysis channel is effective in solid Xe as evidenced by the appearance of the NCO radical absorption around 1916 cm^{-1}.[23,27] This channel establishes a promising starting point for preparing HXeNCO by thermal mobilization of hydrogen atoms. Indeed, new bands appear at 1788.1 and 2148.3 cm^{-1} upon annealing the photolyzed matrix (see Figure 2a) at the mobilization temperature of H atoms (∼45 K) in solid Xe.[28] Upon deuteration, the band at 1788.1 cm^{-1} shifts to 1298.8 cm^{-1} giving a H/D ratio of 1.3767 and the band at 2148.3 cm^{-1} shifts to 2145.4 cm^{-1} as shown in Figure 2b. Intensity of these bands depends on photolysis time and follows roughly the amount of NCO radical which approaches maximum concentration when about 50% of HNCO is decomposed. In longer irradiation, NCO decreases and upon subsequent annealing the intensity of the new bands remains lower. If the matrix is irradiated long enough to bleach NCO almost completely the annealing hardly produces absorptions at 1788.1 and 2148.3 cm^{-1}. These observations suggest that the species responsible for these bands contains the NCO fragment. It should be noted that there are other products growing in the annealing previously identified as HCO, HXeH, H_2NCO, HXeCN, and HXeNC.[23] In the annealing, NCO radical decreases typically by about 40%, and this is attributed to the reaction of NCO with hydrogen atoms to produce the new product. It is notable, however, that the precursor HNCO does not increase in annealing.

A convenient way to separate the bands of different species is to use selective photolysis which exploits differences in the photostabilities of various compounds. We found that irradiation at 405 nm decreases rather selectively the bands at 2148.3 and 1788.1 cm^{-1}. As shown in Figure 3, the difference spectra clearly indicate the decrease of the new species and the simultaneous increase of bands belonging to HNCO (or DNCO) and NCO radical. The signal from NCO is much weaker than HNCO but this is mostly due to the much smaller absorption cross section of NCO compared to HNCO.

Analysis of a representative experiment shows that in the 405 nm photolysis the new compound decomposes to HNCO and H + NCO with the 7:3 branching ratio. The amount of HNCO regenerated corresponds to about 5% of the originally decomposed HNCO at 193 nm. Taking into account the 405 nm photolysis branching ratio and the amount of reacted NCO in annealing, we obtain for this particular experiment that about 18% of decomposed HNCO constituted the H + NCO channel and about 7% of the originally decomposed HNCO was converted to the new product. However, in this experiment the amount of the new product was not necessarily optimal keeping in mind that the concentrations of the products produced in the annealing strongly depend on the extent of irradiation. In addition, we noticed that the product ratios are different for deuterated compounds. In one experiment, the 405 nm photolysis of the new product produced DNCO as much as 24% from the originally decomposed DNCO. This is much more than observed for HNCO, suggesting large differences in the photochemical properties of HNCO and DNCO. However, more detailed analysis is out of the scope of this report.

TABLE 1: MP2/LJ18/6-311++G(2d,2p) Calculated Vibrational Wavenumbers of HXeNCO and HXeOCN[a]

approx mode	HXeNCO	DXeNCO	exp	HXeOCN	DXeOCN
ν_{as}(ABC)	2224.5 (1051)		2148.3 (HXeNCO)	2186.4 (135)	
		2213.3 (1550)	2145.4 (DXeNCO)		2169.3 (463)
ν(Xe−H)	1986.2 (1709)		1788.1, 1793.2[b] (HXeNCO)	2118.3 (906)	
ν(Xe-D)		1417.8 (649)	1298.8, 1302.2[b] (DXeNCO)		1516.0 (294)
ν_s(ABC)	1287.6 (20)	1286.7 (36)		1142.5 (177)	1141.9 (185)
δ(ABC) ip	653.3 (10)	648.0 (6)		620.8 (11)	594.1 (18)
δ(ABC) oop	631.0 (7)	617.2 (12)		573.1 (<1)	549.0 (5)
δ(HXeA) ip	630.7 (<1)	459.2 (4)		556.8 (8)	422.0 (1)
δ(HXeA) oop	616.7 (13)	456.3 (2)		545.5 (6)	412.0 (<1)
ν(XeABC)	325.5 (160)	325.1 (161)		321.9 (130)	320.9 (129)
δ(HXeABC)	55.7 (9)	55.2 (9)		87.9 (10)	86.9 (9)

[a] The numbers in the parentheses are the infrared intensities in km mol^{-1}. In the mode assignment, ABC refers either to NCO or OCN. [b] Sidebands.

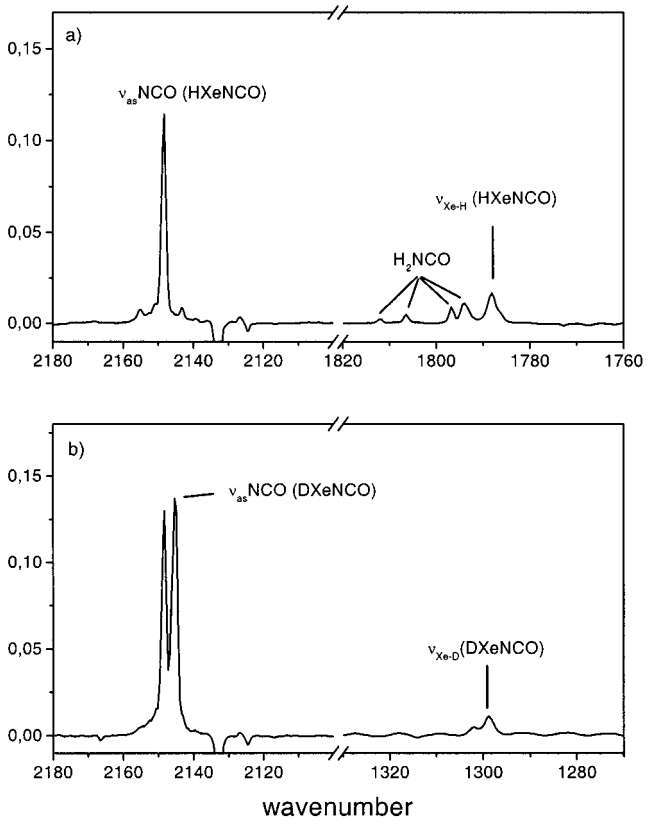

Figure 2. Difference spectra between situations before and after annealing at 50 K of (a) HNCO/Xe = 1/2000 and (b) (HNCO + DNCO)/Xe = 1/2000 matrices after photolysis of the precursor. Note the different wavenumber regions in (a) and (b) in the Xe−H(D) stretching region.

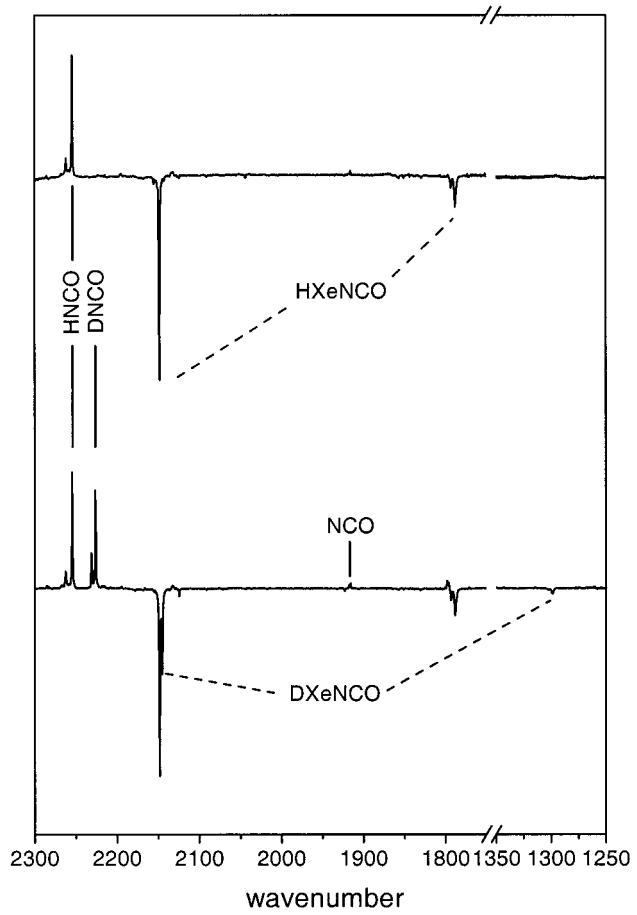

Figure 3. Difference spectra between situations before and after 405 nm irradiation of (a) HNCO/Xe = 1/2000 and (b) (HNCO + DNCO)/Xe = 1/2000 matrices prepared by photolyzing the precursor and annealing at 50 K.

An important observation was made concerning formation of the new product. It was formed not only in annealing but also directly in the photolysis of HNCO. The kinetics of its formation and decomposition under 193 nm photolysis is shown in Figure 4 together with the kinetics of HNCO. The new product rises fast, reaches a maximum, and decreases after that, vanishing finally completely. The concentration of the new product relative to HNCO was obtained from the ratio of the absorption cross sections for HNCO and the new product determined from the 405 nm interconversion experiment. The maximum concentration of the new product during photolysis obtained in this way is about 0.4% from the initial concentration of HNCO. If subsequent annealing is performed at the stage when NCO concentration is near its maximum, the concentration of the new product becomes about an order of magnitude larger. We photolyzed HNCO also with 225, 240, 250, and 266 nm but the formation of the new compound was observed only at 193 nm irradiation. However, at longer wavelengths the amount of NCO was also rather small and it is possible that the amount of the new compound was below our detection limit.

6. Discussion

The experimental observations and the computational results indicate that the new bands appearing in the photolysis of HNCO in solid xenon and upon thermal mobilization of hydrogen atoms belong to HXeNCO. In the following we discuss this assignment in more detail.

In our previous paper[23] we identified the primary photolysis products of HNCO as H + NCO, NH, CO, and NH−CO complexes and these products are to be expected on the basis of the gas-phase photolysis channels.[29] The identification of the new primary product as HXeNCO seems plausible because its

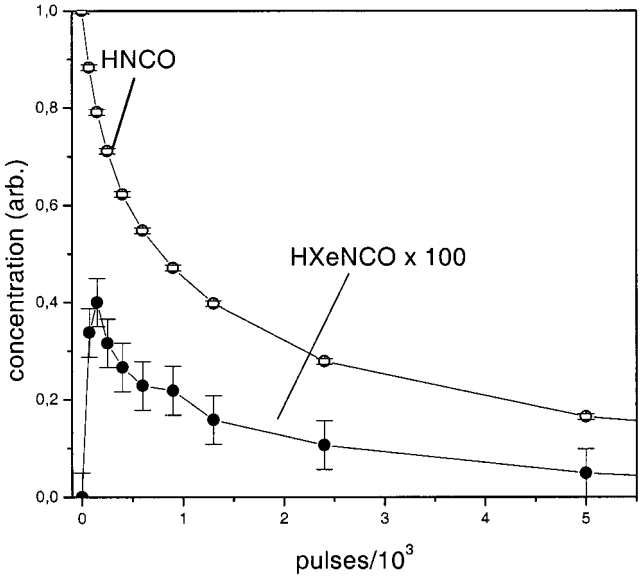

Figure 4. Kinetics of HNCO and HXeNCO under 193 nm irradiation obtained by integration of the relevant IR bands.

formation requires basically only dissociation of the H−N bond of HNCO in a Xe cage and migration of the hydrogen atom out of the parent cage. Of course, HXeOCN is possible as well. The new bands cannot be assigned to isomers of HNCO like HOCN or HCNO.[30] The formation of the new product upon thermal mobilization of the hydrogen atoms further supports the assignment to HXeNCO or HXeOCN since this method has previously been the principal way of synthesizing analogous compounds.[2−7] In addition, since NCO decreases in the annealing but HNCO does not increase there must be another product formed from H and NCO.

The deuteration experiments show that the compound under discussion contains a hydrogen atom and the H/D ratio is suitable for a Xe−H stretch. The shift of the asymmetric NCO stretch by 2.9 cm^{-1} upon deuteration is in a qualitative agreement with the calculations. The photodecomposition of the compound at 405 nm radiation suggests that the species has low-lying dissociative excited states which agrees with our experience on similar compounds.[2−7] Very strong evidence in favor of the assignment comes from the two observed photodissociation channels of the compound which lead to formation of HNCO and NCO. These channels are naturally explained by a rearrangement process leading to HNCO and the escape of H atom leading to NCO. On the other hand, formation of HNCO at 405 nm distinguishes HXeNCO from other HXY molecules. Previously, we never observed recovery of the precursors in photolysis of HXY molecules with a possible exception of HKrCN.[4]

The experiments support the assignment of the new species to either HXeNCO or HXeOCN, and the final task is to choose between these two candidates. Here we rely strongly on the computations. All the evidence suggests the assignment to HXeNCO. The position of the 1788.1 cm^{-1} band is in a perfect agreement with the 1770 cm^{-1} prediction for HXeNCO but far from 1950 cm^{-1} derived for HXeOCN. Calculations give two strong bands for HXeNCO and one strong and two bands of intermediate intensity for HXeOCN. Although the experimental intensity ratio of the Xe−H stretch and asymmetric NCO stretch is different from the computed values, the observations fit better to HXeNCO than to HXeOCN. We did not see any band around 1140 cm^{-1} which would support HXeOCN. Finally, it is more understandable if only the lowest-energy form is observed than if only the highest-energy form is observed, and the latter case seems improbable.

TABLE 2: Computed Structural Parameters of HXeNCO and FXeNCO (Notation AXeNCO)

	HXeNCO[a]	FXeNCO[b]
r(A−Xe)/Å	1.675	2.024
r(Xe−N)/Å	2.326	2.206
r(N−C)/Å	1.215	1.194
r(C−O)/Å	1.193	1.231
∠(A−Xe−N)/deg	178.4	178.7
∠(Xe−N−C)/deg	125.4	125.4
∠(N−C−O)/deg	177.6	174.2

[a] This work (MP2/LJ18/6-311++G(2d,2p)), see text for details. [b] From ref 10 (MP2/LANL2DZ/6-31G(d)).

SCHEME 1

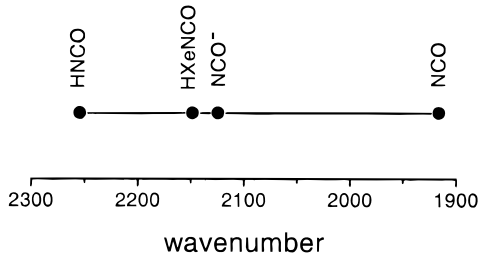

Altogether, the facts presented above make us assign the new bands to HXeNCO. It is somewhat bothersome that we did not find any evidence for the formation of HXeOCN, although it is calculated to be stable. For comparison, in previous experiments with HCN we obtained both HXeCN and HXeNC isomers.[4] It may be that the trapping configuration of NCO favors the HXeNCO channel and that formation of HXeOCN requires larger lattice rearrangement, which can introduce higher barrier for the formation of HXeOCN compared with HXeNCO.

Table 2 compares the computed structures of HXeNCO and FXeNCO. Schulz and Klapötke obtained exactly the same Xe−N−C angle for FXeNCO[10] as we obtain for HXeNCO, and also other parameters are rather similar. The largest difference is that the Xe−N distance in FXeNCO is 2.21 Å which is somewhat shorter than in HXeNCO and this may be an indication of larger covalent contributions in FXeNCO compared with HXeNCO. Qualitatively, this can be understood by the strong admixture of the $F^-(XeNCO)^+$ resonance structure in FXeNCO in addition to the more dominating $(FXe)^+NCO^-$ structure. In HXeNCO, the $(HXe)^+NCO^-$ resonance structure is more dominating. Schultz and Klapötke also predicted FXeOCN to be the higher energy isomer similarly to our case. It is interesting to note that their experiments show indirectly the formation of FXeNCO but not FXeOCN bearing some similarity to our observations regarding HXeNCO and HXeOCN.

Comparison of the NCO stretching wavenumbers of different compounds is shown in Scheme 1. It is possible to obtain some information on the nature of HXeNCO by comparing its NCO stretching wavenumber with HNCO, NCO, and NCO^-. The HXeNCO absorption is very far from the absorption of NCO in Xe, and this emphasizes the fact that HXeNCO is *not* a van der Waals complex between H, Xe, and NCO. If, on the other hand, HXeNCO was a complete ion pair $(HXe)^+(NCO)^-$ the NCO stretch should be near the free NCO^- value. HNCO can be taken as an example of a covalently bound system and inclusion of covalent bonding in HXeNCO should shift the NCO stretch toward the HNCO value. On this basis, the bonding in HXeNCO is dominated by ionic character but some covalent effects are found as well. This picture seems to be in accordance with the description provided by ab initio calculations.

The decrease of NCO by about 40% in the annealing due to reaction with hydrogen atoms indicates that the amount of hydrogen atoms stabilized in the lattice after photolysis is comparable to the amount of NCO radicals. Especially, when all the other species produced from hydrogen atoms (XeH_2, H_2-NCO, etc.) are taken into account, we can conclude that there are no significant losses of H atoms during photolysis. This estimate is in contradiction with the results from photodissociation of hydrogen halides in solid Xe of refs 14 and 16 where it was stated that due to long distance photoinduced migration, H atoms undergo secondary reactions leading to dramatic losses of H atoms during photolysis. Our current results do not support long distance photomigration or significant loss channels for H atoms in agreement with our previous observations.[4,8]

From the dynamical point of view, the formation of HXeNCO directly in the 193 nm photolysis of HNCO is the most interesting observation. At least two alternatives for the mechanism of formation of HXeNCO are possible: First, HXeNCO can be formed directly from HNCO/Xe in a photoisomerization process, or it can be formed as a result of trapping of H in a HXeNCO form after extensive sampling of the multidimensional potential energy surface of the system and after loosing enough kinetic energy. Second, there is a possibility that hydrogen atom is trapped nearby NCO after photolysis of HNCO after which it can be activated to form HXeNCO, for example, by 193 nm induced H−Xe charge-transfer excitation.[31] The exact mechanism of the photoinduced formation of HXeNCO cannot be deduced from these experiments but, in any case, its formation shows that HXeNCO form must be taken into account when describing the photodissociation of HNCO in solid Xe. Intuitively, the formation of HXeNCO is a very natural process because HXeNCO configuration represents a deep potential energy minimum for the hydrogen atom and some portion of them should be trapped in HXeNCO irrespective of the exact mechanism. The formation of HXeNCO has important consequences with respect to the distribution of hydrogen atoms after photodissociation of HNCO. Once formed, photolysis of HXeNCO provides much more kinetic energy to the hydrogen atom than the direct dissociation of HNCO at the same wavelength. Here, we see that ignorance of formation of HXeNCO may lead to false conclusions concerning the relation between the kinetic energy of the hydrogen atom and its migration distance.

We have all the reasons to suggest that the sequence of events leading to the dissociation of a hydride in solid Xe is not limited to the case of HNCO. Rather, the intermediate formation of HXY form can be expected to be general. We suppose that a reason for the previous lack of observation of the formation of HXY compounds in photolysis of HY is the efficient decomposition of HXY under irradiation. In this case, the steady-state concentration of HXY remains too low to be detected. In the case of HXeNCO, the ratio of the rate of formation and decomposition is fortunately large enough to allow the detection.

7. Conclusions

A novel rare-gas compound HXeNCO has been characterized experimentally in solid xenon by FTIR spectroscopy and computationally by ab initio calculations. The deuteration experiments fully support the assignment. HXeNCO has two strong absorptions: asymmetric NCO stretch at 2148.3 cm^{-1} and Xe−H stretch at 1788.1 cm^{-1}. HXeNCO can be generated by photolyzing HNCO into H atoms and NCO radicals and posterior thermal mobilization of H atoms, which leads to the formation of HXeNCO via reaction H + Xe + NCO → HXeNCO. The compound photodecomposes at 405 nm irradiation forming HNCO and (NCO + H). Additionally and importantly, the experimental evidence suggests that HXeNCO is formed in the 193 nm photolysis indicating that HXY compounds can act as intermediates in the photolysis of HY in solid X. This experimental fact shows that any realistic modeling of such dynamical processes should take into account the existence of HXY.

Acknowledgment. This project was supported by the Academy of Finland. The CSC-Center for Scientific Computing Ltd. (Espoo, Finland) is thanked for providing mainframe computer time.

References and Notes

(1) For a recent review, see: Holloway, J. H.; Hope, E. G. *Adv. Inorg. Chem.* **1999**, *46*, 51.
(2) Pettersson, M.; Lundell, J.; Räsänen, M. *J. Chem. Phys.* **1995**, *102*, 6423.
(3) Pettersson, M.; Lundell, J.; Räsänen, M. *J. Chem. Phys.* **1995**, *103*, 205.
(4) Pettersson, M.; Lundell, J.; Khriachtchev, L.; Räsänen, M. *J. Chem. Phys.* **1998**, *109*, 618.
(5) Pettersson, M.; Lundell, J.; Khriachtchev, L.; Isoniemi, E.; Räsänen, M. *J. Am. Chem. Soc.* **1998**, *120*, 7979.
(6) Pettersson, M.; Lundell, J.; Räsänen, M. *Eur. J. Inorg. Chem.* **1999**, 729.
(7) Pettersson, M.; Khriachtchev, L.; Lundell, J.; Räsänen, M. *J. Am. Chem. Soc.* **1999**, *121*, 11904.
(8) Pettersson, M.; Nieminen, J.; Khriachtchev, L.; Räsänen, M. *J. Chem. Phys.* **1997**, *107*, 8423.
(9) Bradforth, S. E.; Kim, E. H.; Arnold, D. W.; Neumark, D. M. *J. Chem. Phys.* **1993**, *98*, 800.
(10) Schulz, A.; Klapötke, T. M. *Inorg. Chem.* **1997**, *36*, 1929.
(11) Lawrence, W.; Okada, F.; Apkarian, V. A. *Chem. Phys. Lett.* **1988**, *150*, 339.
(12) LaBrake, D.; Weitz, E. *Chem. Phys. Lett.* **1993**, *211*, 430.
(13) Kunttu, H. M.; Seetula, J. *Chem. Phys.* **1994**, *189*, 273.
(14) LaBrake, D.; Ryan, E. T.; Weitz, E. *J. Chem. Phys.* **1995**, *102*, 4112.
(15) Gödderz, K. H.; Schwentner, N.; Chergui, M. *J. Chem. Phys.* **1996**, *105*, 451.
(16) Eloranta, J.; Vaskonen, K.; Kunttu, H. *J. Chem. Pys.* **1999**, *110*, 7917.
(17) Apkarian, V. A.; Schwentner, N. *Chem. Rev.* **1999**, *99*, 1481.
(18) Alimi, R.; Gerber, R. B.; Apkarian, V. A. *J. Chem. Phys.* **1988**, *89*, 174.
(19) Gerber, R. B.; Alimi, R. *Chem. Phys. Lett.* **1990**, *173*, 393.
(20) Gersonde, I. H.; Gabriel, H. *J. Chem. Phys.* **1993**, *98*, 2094.
(21) Jungwirth, P.; Gerber, R. B. *J. Chem. Phys.* **1995**, *102*, 6046.
(22) Schröder, T.; Schinke, R.; Liu, S.; Bačić, Z.; Moskowitz, J. W. *J. Chem. Phys.* **1995**, *103*, 9228.
(23) Pettersson, M.; Khriachtchev, L.; Jolkkonen, S.; Räsänen, M. *J. Phys. Chem. A.* **1999**, *103*, 9154.
(24) Frisch, M. J.; Trucks, G. W.; Schlegel, H. B.; Scuseria, G. E.; Robb, M. A.; Cheeseman, J. R.; Zakrzewski, V. G.; Montgomery, J. A. Jr.; Stratmann, R. E.; Burant, J. C.; Dapprich, S.; Millam, J. M.; Daniels, A. D.; Kudin, K. N.; Strain, M. C.; Farkas, O.; Tomasi, J.; Barone, V.; Cossi, M.; Cammi, R.; Mennucci, B.; Pomelli, C.; Adamo, C.; Clifford, S.; Ochterski, J.; Petersson, G. A.; Ayala, P. Y.; Cui, Q.; Morokuma, K.; Malick, D. K.; Rabuck, A. D.; Raghavachari, K.; Foresman, J. B.; Cioslowski, J.; Ortiz, J. V.; Stefanov, B. B.; Liu, G.; Liashenko, A.; Piskorz, P.; Komaromi, I.; Gomperts, R.; Martin, R. L.; Fox, D. J.; Keith, T.; Al-Laham, M. A.; Peng, C. Y.; Nanayakkara, A.; Gonzalez, C.; Challacombe, M.; Gill, P. M. W.; Johnson, B.; Chen, W.; Wong, M. W.; Andres, J. L.; Gonzalez, C.; Head-Gordon, M.; Replogle, E. S.; and Pople, J. A. *Gaussian 98*, Revision A.3; Gaussian, Inc.: Pittsburgh, PA, 1998.
(25) LaJohn, L. A.; Christiansen, P. A.; Ross, R. B.; Atashroo, T.; Ermler, W. C. *J. Chem. Phys.* **1987**, *87*, 2812.
(26) Lundell, J.; Pettersson, M.; Räsänen, M. *Comput. Chem.*, in press.
(27) Milligan, D. E.; Jacox, M. E. *J. Chem. Phys.* **1967**, *47*, 5157.
(28) Feldman, V. I.; Sukhov, F. F.; Orlov, A. Yu. *Chem. Phys. Lett.* **1997**, *280*, 507.
(29) Zyrianov, M.; Droz-Georget, Th.; Reisler, H. *J. Chem. Phys.* **1999**, *110*, 2059.
(30) Teles, J. H.; Maier, G.; Hess, B. A.; Schaad, L. J.; Winnewisser, M.; Winnewisser, B. P. *Chem. Ber.* **1989**, *122*, 753.
(31) Creuzburg, M.; Wittl, F. *J. Mol. Struct.* **1990**, *222*, 127.